Attitude Determination Using Multiple L1 GPS Receivers

João Cóias
Instituto Superior Técnico, Technical University of Lisbon, Portugal
joao.coias@ist.utl.pt

Abstract— **GPS based techniques allow a highly accurate attitude determination when using carrier phase measurements. However, these techniques require the determination of the integer carrier phase ambiguities. This is a problem that is usually addressed in a context of dual frequency receivers. Due to the high cost of these receivers, strong motivation exists to explore these techniques with cheaper L1 single frequency receivers. In this paper, two high accuracy attitude determination techniques are proposed, one using a Least Squares estimation algorithm and the rotation matrix, and the second one using the rotation quaternion that is determined resorting to an Extended Kalman Filter. The observations are based on multiple baselines, using low cost single frequency L1 GPS receivers. Both techniques allow the attitude determination with precisions smaller than 1°. Test results with real data are presented.**

Keywords – Ambiguity Filter, attitude determination, double differences, GPS, integer ambiguity, LAMBDA method.

I. INTRODUCTION

GPS based attitude determination can be accomplished by using at least three receivers and calculating the baseline vectors between the reference receiver antenna and each auxiliary antenna. To achieve highly accurate baseline vectors carrier phase measurements have to be used and hence the carrier phase integer ambiguities have to be determined. Techniques with dual frequency L1/ L2 GPS receivers provide a quick and robust way for integer ambiguity resolution. However, for single frequency L1 receivers the problem is harder, see, [1-3] and the references therein. The motivation to work with single frequency GPS receivers arises from the high cost of the dual frequency receivers. Thus, in this paper a technique to solve the attitude is proposed based on the use of multiple L1 GPS receivers.

For integer ambiguity resolution, several techniques have been proposed, but the one that collects most credits is the LAMBDA method, see, [4-6]. However, for multiple baselines fixed on a body frame, the LAMBDA method's outputs do not respect the constraints given by the problem's geometry. There are some evolutions possible for this technique aiming to incorporate the constraints explicitly, as advanced in [7] and [8]. These techniques use the constraints to improve the search process in the LAMBDA method. The approach used in this paper was to work with the LAMBDA method's outputs and then filter the best integer ambiguity solution using the Ambiguity Filter proposed in, [9-12].

Improvements to the Ambiguity Filter are proposed to increase the confidence in the selected integer ambiguity. For the attitude determination, multiple baselines, fixed with the vehicle body frame, will be used.

The rest of the paper is structured as follows. In Section II the system, its observables and the relation with the baseline vectors are defined. The techniques used to solve the integer ambiguity problem are the main focus of Section III. The techniques used to solve the attitude determination problem based on multiple baselines are presented in Section IV. Section V addresses the more practical topics regarding the implementation of the developed techniques. Section VI shows the results of the field tests, which lead to the conclusions presented in Section VII.

II. SYSTEM DEFINITION

A. Introduction

The determination of the baseline vector is done by using interferometric techniques. This consists on the differentiation of measurements from two receivers. Thus, in the GPS case this leads to carrier phase and code (pseudoranges) double differences, which are used as observations in the developed system. These observables are introduced next.

B. Single and Double Differences

Generation of both carrier-phase and code double differences ($\nabla\Delta$) can be used in the determination of the baseline vector between two GPS receivers, one used as reference station and the second used as auxiliary station. In the case of multiple receivers, the correct synchronization of all measurements is mandatory. The computation of these double differences is done in two steps. The first one corresponds to differentiating the measurements for a given same satellite, provided by two receivers, which are called single differences (Δ). Thus, for the satellite p and receiver k, one must have the following phase measurements:

$$\Phi_k^p = \rho_k^p + \lambda N_k^p + c\left(t_p + t_k + T_k^p + I_k^p\right) + \epsilon_k^p \tag{1}$$

where

- Φ_k^p is the measured carrier phase (in meters);
- ρ_k^p is the geometric range between the receiver k and the satellite p (in meters);
- λ is the carrier wavelength (in meters);
- N_k^p is the carrier phase integer ambiguity (in cycles);
- c is the speed of light in vacuum (in meters per second);

- t_p and t_k are the satellite and the receiver clock offset (in seconds), respectively;
- T_k^p and I_k^p are the tropospheric and ionospheric delays (in seconds), respectively;
- ϵ_k^p modes the disturbance noise due to different factors (hardware, multipath).

Adding a receiver m, one is able to form the aforementioned single differences, represented by,

$$\begin{aligned}\Delta\Phi_{km}^{p} &= \Phi_k^p - \Phi_m^p = \\ &= \Delta\rho_{km}^{p} + \lambda\Delta N_{km}^{p} + c\Delta t_{km} + \Delta\epsilon_{km}^{p}.\end{aligned} \tag{2}$$

It is possible to verify that the clock offset of the satellite is cancelled. The same happens to the common tropospheric and ionospheric errors, which are assumed to have equal magnitude in the measurements of both receivers. This assumption is possible in the case where the distance between the receivers is small (less than 50 km, accordingly with [2]) when compared with the satellite-receiver distance. However, this process does not eliminate the receiver clock offset.

The double differences are obtained with the difference between two single differences. Considering the satellite q and the equation (2), the double differences are given by

$$\begin{aligned}\nabla\Delta\Phi_{km}^{pq} &= \Delta\Phi_{km}^{p} - \Delta\Phi_{km}^{q} = \\ &= \nabla\Delta\rho_{km}^{pq} + \lambda\nabla\Delta N_{km}^{pq} + \nabla\Delta\epsilon_{km}^{pq}.\end{aligned} \tag{3}$$

This operation eliminates the receiver clock offset.

For code measurements, that are given by an expression similar to (1) but without the ambiguity term, the determination of the double differences is analogous to the one presented in (2) and (3). So, double differences for code measurements are given by

$$\begin{aligned}\nabla\Delta PR_{km}^{pq} &= \Delta PR_{km}^{p} - \Delta PR_{km}^{q} = \\ &= \nabla\Delta\rho_{km}^{pq} + \nabla\Delta\epsilon_{km}^{pq}.\end{aligned} \tag{4}$$

C. Observation Model

In order to determine the baseline vector between two antennas, it is necessary to relate it with the double differences defined above. Using interferometric techniques, it is clear that the projection of the baseline onto the line of sight (LoS) between the satellite and the receiver can be represented by the inner product of b with the direction cosine unit vector e^p. This projection of b is the single difference range between the receivers k and m relative to the satellite p. Thus, single differences of range can be represented as

$$\Delta\rho_{km}^{p} = b \cdot e^{p}. \tag{5}$$

The formation of double differences range is straightforward and given by

$$\nabla\Delta\rho_{km}^{pq} = b \cdot (e^{p} - e^{q}) = b \cdot e^{pq}. \tag{6}$$

The determination of the direction cosines e^p and e^q is done by computing the user position and the respective satellite position. Note that, since the receiver-satellite distance is much bigger than the baseline length, it is assumed that a satellite's direction cosine is equal to both receivers.

At this point it is possible to formulate the system that relates the baseline vector and the integer ambiguities with the observed double differences. Thus, for a constellation of n satellites the system is defined as

$$\begin{bmatrix}\nabla\Delta PR_{km}^{12}\\ \nabla\Delta PR_{km}^{13}\\ \vdots\\ \nabla\Delta PR_{km}^{1n}\\ \nabla\Delta\Phi_{km}^{12}\\ \nabla\Delta\Phi_{km}^{13}\\ \vdots\\ \nabla\Delta\Phi_{km}^{1n}\end{bmatrix} = \begin{bmatrix} e_{km_x}^{12} & e_{km_y}^{12} & e_{km_z}^{12}\\ e_{km_x}^{13} & e_{km_y}^{13} & e_{km_z}^{13}\\ \vdots & \vdots & \vdots\\ e_{km_x}^{1n} & e_{km_y}^{1n} & e_{km_z}^{1n}\\ e_{km_x}^{12} & e_{km_y}^{12} & e_{km_z}^{12}\\ e_{km_x}^{13} & e_{km_y}^{13} & e_{km_z}^{13}\\ \vdots & \vdots & \vdots\\ e_{km_x}^{1n} & e_{km_y}^{1n} & e_{km_z}^{1n}\end{bmatrix}\begin{bmatrix}b_x\\ b_y\\ b_z\end{bmatrix} \dots$$

$$+\begin{bmatrix}0 & 0 & \cdots & 0\\ 0 & 0 & \cdots & 0\\ \vdots & \vdots & \ddots & \vdots\\ 0 & 0 & \dots & 0\\ \lambda & 0 & \dots & 0\\ 0 & \lambda & \dots & 0\\ \vdots & \vdots & \ddots & \vdots\\ 0 & 0 & 0 & \lambda\end{bmatrix}\begin{bmatrix}\nabla\Delta N_{km}^{12}\\ \nabla\Delta N_{km}^{13}\\ \vdots\\ \nabla\Delta N_{km}^{1n}\end{bmatrix} + \begin{bmatrix}\nabla\Delta\epsilon_{km}^{12}\\ \nabla\Delta\epsilon_{km}^{13}\\ \vdots\\ \nabla\Delta\epsilon_{km}^{1n}\\ \nabla\Delta\epsilon_{km}^{12}\\ \nabla\Delta\epsilon_{km}^{13}\\ \vdots\\ \nabla\Delta\epsilon_{km}^{1n}\end{bmatrix}. \tag{7}$$

Note that the superscript 1 represents the reference satellite, selected as the one with highest elevation angle. This choice is done to optimize the geometry and reduce the system dilution of precision (DOP), [9].

The system defined above can be reduced to the form

$$y = Bb + Aa + e, \tag{8}$$

where,

- y is the observed vector of double differences ($\mathbb{R}^{2(n-1)\times 1}$);
- B is the system matrix for the baseline coordinates, containing the differenced direction cosines ($\mathbb{R}^{2(n-1)\times 3}$);
- b is the baseline coordinates' vector ($\mathbb{R}^{3\times 1}$);
- A is the system matrix for the integer ambiguity set ($\mathbb{R}^{2(n-1)\times(n-1)}$);
- a is the aforementioned integer ambiguity set ($\mathbb{R}^{(n-1)\times 1}$);
- e is the measurement noise vector, assumed to have Gaussian distribution, with expected value zero and covariance matrix Q_y, which is symmetric and positive defined, [4]. Since double differences are correlated, Q_y is not a diagonal matrix.

Defining the augmented system matrix $H = [A \quad B]$, with dimension $2(n-1) \times (n-1) + 3$, one would have an augmented state vector $x = [a^T \quad b^T]^T$, with dimension $(n-1) + 3 \times 1$. Analyzing the augmented system, it is possible to conclude that there are enough equations to estimate all the states (i.e. baseline vector and integer ambiguities), if the full rank of the matrix H is equal to the number of states, that is, $(n-1) + 3$. This is only verified when the constellation has, at least, four satellites, i.e. $n \geq 4$.

III. Baseline determination And Integer Ambiguity Resolution

A. Float Solution

The solution for the system (8) can be determined resorting to a weighted least squares estimator, in order to minimize the error norm defined as, [6],

$$\|y - Bb - Aa\|^2_{Q_y^{-1}}, \tag{9}$$

where $\|e\|^2 = e^T Q_y^{-1} e$. Thus, the estimator should be represented by

$$\begin{bmatrix}\hat{a}\\ \hat{b}\end{bmatrix} = \left([A \quad B]^T Q_y^{-1}[A \quad B]\right)^{-1}[A \quad B]^T Q_y^{-1} y. \tag{10}$$

Despite the error minimization, the estimator gives a floating point solution but in general it is not the most appropriated, since the correct ambiguities are integers. The correct baseline coordinates can only be obtained with the correct integer ambiguities. The best way to correctly determine the integer ambiguities is using search techniques.

B. Code Smoothing

Based on the Kalman Filter (KF), introduced by [13], the code smoothing makes use of the combination between the noisy code double differences and the less noisy carrier-phase double differences with a Complementary KF, [14]. The technique uses the average of the noisier measurement to center the quieter one, limiting the size of the integer ambiguity. Thus, the filter's output, at instant k, is a smoothed (less noisier) code double difference, $\nabla\Delta S$. For that, the filter has the form

$$\nabla\Delta S_k^- = \nabla\Delta S_{k-1}^+ + (\nabla\Delta\phi_k - \nabla\Delta\phi_{k-1}), \tag{11}$$

$$P_k^- = P_{k-1}^+ + cov(\nabla\Delta\phi), \tag{12}$$

$$K_k = P_k^-(P_k^- + cov(\nabla\Delta PR))^{-1}, \tag{13}$$

$$\nabla\Delta S_k^+ = \nabla\Delta S_k^- + K_k(\nabla\Delta PR_k - \nabla\Delta S_k^-), \tag{14}$$

$$P_k^+ = (I - K_k)P_k^-. \tag{15}$$

Equations (11) and (12) compose the prediction step. In the first one, the smoothed code double differences are propagated from the previous instant with the change rate of the carrier-phase double differences. By differencing two carrier-phase double differences the integer ambiguity is canceled, and hence the propagated $\nabla\Delta S_k^-$ is unambiguous. In the second line the, the error covariance matrix is obtained by adding the new covariance matrix of the carrier phase double differences to the previous error covariance matrix.

For the update step, the Kalman gain is calculated as described in equation (13). In the equation (14), the predicted smoothed code double differences are propagated with the weighted residual between the measured code double differences and the smoothed code double differences. Finally, in equation (15) the estimation error covariance is propagated to the new instant, maintaining the balance between the unambiguous but noisier code measurements and the ambiguous but smoother carrier phase measurements.

C. LAMBDA Method

From all the existing search techniques in the ambiguity domain, the LAMBDA method (Least-Squares AMBiguity Decorrelation Adjustment) proposed in [4], is considered to be the most efficient one, accordingly to [6] and [15], So, it was chosen as the search technique to use in this work and it will be presented in detail. It is composed of three steps: float solution, integer ambiguity estimation, and fixed solution, [5].

In the float solution step, the inaccurate solution obtained by the weighted least squares estimator, $\hat{a}$ in equation (10), is used in the search process as the central point. The error estimation covariance matrix, $Q_{\hat{a}}$, defines the search space to find the correct integer ambiguity vector, $\check{a}$, that minimizes the cost function $\|\hat{a} - a\|^2_{Q_{\hat{a}}}$, given by,

$$\check{a} = arg\left(min_{a\in\mathbb{Z}}\|\hat{a} - a\|^2_{Q_{\hat{a}}}\right), \tag{16}$$

that is the integer ambiguity estimation step.

Due to the correlated nature of double differences (which leads to a non diagonal covariance matrix for double differences and, consequently, a non diagonal covariance matrix for the float solution) the search space is in general elliptical. The LAMBDA method uses a transformation matrix to decorrelate the error and, therefore, to diagonalize the covariance matrix of the float solution, creating a search space that is nearly spherical. This diagonalization is accomplished by a Z transformation defined as

$$Q_{\hat{z}} = Z^T Q_{\hat{a}} Z. \tag{17}$$

The next step is to decompose the covariance matrix of the float solution as

$$Q_{\hat{a}} = L^T D L, \tag{18}$$

where L is a lower matrix and D is a diagonal matrix. Knowing that the elements of Z are integers and that Z is close to L^{-1} one must have

$$Q_{\hat{z}} = \tilde{L}^T \tilde{D} \tilde{L}, \tag{19}$$

where the non diagonal elements of this new covariance matrix, represented by $\tilde{L}$, are close to zero, leading to a nearly diagonal covariance matrix.

After this decorrelation process, the new cost function is,

$$\check{z} = arg\left(min_z\|\hat{z} - z\|^2_{Q_{\hat{z}}}\right), \tag{20}$$

where $z = Z^T a$ and $\hat{z} = Z^T \hat{a}$, and hence the fixed solution is $\check{a} = Z^{-T}\check{z}$.

The volume of the search space is controlled by the value χ^2 that takes into account the new nearly diagonal covariance matrix and the number of candidates desired by the user. That is, the LAMBDA method outputs those ambiguities that verify the inequality

$$(\hat{z} - z)^T Q_{\hat{z}}{}^{-1}(\hat{z} - z) \leq \chi^2. \tag{21}$$

Note that the outputs are sorted in the ascending order of distance to the float solution.

D. Ambiguity Filter

Following the methodology developed in [9], the Ambiguity Filter developed in this paper chooses the best ambiguity set from the outputs from the LAMBDA method. For each candidate set $\check{a}$, as resulting from LAMBDA method, the correspondent baseline, $\check{b}(\check{a})$, is computed with the objective of assigning merit to each candidate.

The Ambiguity Filter is composed by three steps: validation, selection, and stabilization. Before the description of these three steps, the process of merit assignment will be described.

1) Merit Attribution

Three types of tests were used in the merit attribution. The first two, also presented in [9], were the residual ratio and the baseline length constraint. The third one, proposed in this paper, makes use of the Up coordinate while the ambiguity set is not stabilized.

a) Residual Ratio

For each candidate and the respective baseline solution, the phase residual vector V is calculated as the difference between the estimated phase double differences and the measured ones. That is, the phase residual vector is given by

$$V = B\check{b} + A\check{a} - \nabla\Delta\Phi, \qquad (22)$$

and its Euclidean norm is obtained by

$$\|V\|^2 = V^T\left(cov(\nabla\Delta\Phi)\right)^{-1}V. \qquad (23)$$

The ambiguity set with smaller phase residual error will be the one with higher merit.

b) Baseline Length Constraint

With the knowledge of the real baseline distance, l, the error of the estimated baseline is obtained as

$$\delta_b = \left|\|\check{b}(\check{a})\| - l\right| \qquad (24)$$

c) Up Coordinate Constraint

This test is similar to the previous one, but only considers the Up coordinate resulting from the candidate set that is being tested. It is assumed that during the initialization (i.e. while there is no stabilized solution) the platform is stopped, which leads to a constant baseline vector. By measuring the altitude difference between the reference antenna and the auxiliary one, it is possible to obtain the real Up coordinate, u_{real}. Thus, the Up coordinate error is given by

$$\delta_u = |\check{u}(\check{a}) - u_{real}|. \qquad (25)$$

For each of the three tests defined above, the errors of the candidates are grouped in a vector with ascending order of the respective error, which is the descending order of merit. So, the merit, M, of a candidate set will be attributed according with position, i, of the error in the sorted vector, that is

$$M_i = 1/i. \qquad (26)$$

2) Validation

The validation step makes use of the baseline length error, described by equation (24), and defining a threshold that was set to be $10\,cm$, due do the errors present in the baseline estimation. That is,

$$\delta_b = \left|\|\check{b}(\check{a})\| - l\right| \leq 0.1 \qquad (27)$$

The candidates that have a baseline length error bigger than the threshold are excluded.

3) Selection

This step is where the merit is assigned. This is done by combining two of the tests defined previously in two different metrics:

1. residual ratio and baseline length constraint;
2. baseline length constraint and Up coordinate constraint.

The candidate set with higher merit, using the metric 1 or the metric 2, will be selected as the fixed solution for the respective epoch.

4) Stabilization

The candidate set selected as the fixed solution by the Ambiguity Filter in each epoch, is stored in a data base. As debated in [9], the ambiguity set that first achieves 50 occurrences as a fixed solution (i.e. a candidate is selected as the fixed solution in 50 different epochs) is the optimal fixed solution. Thereafter the optimal baseline vector will be determined by the optimal fixed solution.

In dynamic environments variations in the satellite constellation occur quite often (i.e. change of the reference satellite, loss of lock, cycle slips). The algorithm proposed in this paper uses the same constellation in the maximum number of epochs. Even if a new satellite becomes visible, the algorithm uses those satellites for which the integer ambiguity is known. When the number of satellites falls to less than four, the algorithm uses the last baseline's estimate (i.e. calculated using the optimal ambiguity set) and recovers the ambiguity set for the new constellation. Then the recovered ambiguity set is used to calculate the present baseline vector. This adaptation to a new constellation represents an improvement in the use of the Ambiguity Filter.

The correction of other phenomenon that affect the integrity of the baseline solution, such as cycle slips and change of the reference satellite, is done as described in [9].

IV. Attitude Determination

A. Introduction

Using the Ambiguity Filter in the determination of multiple baselines it is possible to solve the attitude determination problem. In this paper three baselines (i.e. four GPS receivers) were used. Thus, two techniques regarding the attitude determination are proposed. First, a simple technique using rotation matrices is presented. Finally, a more complex solution using a rotation quaternion and an Extended Kalman Filter (EKF) is proposed.

B. Attitude Determination Using a Rotation Matrix

As discussed in [2] and [14], among many possible solutions assume that the attitude is defined by the rotation transformation which relates a coordinate system fixed in space (North East Down – NED) to a coordinate system fixed in the body (XYZ: X – pointing in the moving direction; Z – point down; Y – orthogonal to the plane XZ). Due to its nature, the coordinates of the baselines will be constant in the XYZ frame.

The rotation of the body fixed frame can be represented as a series of rotations in the three axis XYZ, that is

$$Rot(\psi,\theta,\phi) = Rot_z(\psi)Rot_y(\theta)Rot_x(\phi) \tag{28}$$

where θ, ϕ and ψ are the attitude angles, respectively, pitch, roll and heading.

Thus, the transformation from the body fixed frame to the space frame is given by

$$B_{NED} = Rot(\psi,\theta,\phi)B_{xyz} \tag{29}$$

where B_{NED} and B_{xyz} are matrices of baselines (as column vectors) in the respective frame.

By solving (29) as a simple Least Squares problem, the rotation matrix $Rot(\psi,\theta,\phi)$ is calculated as

$$Rot(\psi,\theta,\phi) = B_{NED}B_{xyz}^T\left(B_{xyz}B_{xyz}^T\right)^{-1}. \tag{30}$$

From the rotation matrix, defined in (28), the attitude angles can be obtained as represented in (31), where the subscript in the rotation matrix represents its index.

$$\begin{aligned}\theta &= sin^{-1}(-Rot_{31}),\\ \phi &= sin^{-1}\left({Rot_{32}}/{\cos(\theta)}\right),\\ \psi &= cos^{-1}\left({Rot_{11}}/{\cos(\theta)}\right).\end{aligned} \tag{31}$$

This approach has singularities for pitch angles of $\pm 90°$. However, it is easy to obtain the attitude angles for situations where such attitude is not experienced. For a more robust and stable implementation, quaternions may be used.

C. *Quaternion-Based Extended Kalman Filter for Attitude Determination*

1) Quaternion and Euler Angles

As described in [16], instead of rotation matrices, a quaternion may be used as rotation operator. A quaternion is a hyper-complex number of rank 4, and it is defined as

$$q = q_0 + iq_1 + jq_2 + kq_3,. \tag{32}$$

where q_0 is called the scalar part and $iq_1 + jq_2 + kq_3$ are called the vector part. An important property is that the quaternion q is unitary, that is,

$$\|q\|^2 = q_0^2 + q_1^2 + q_2^2 + q_3^2 = 1,. \tag{33}$$

which consists in a crucial constraint when using a quaternion for attitude determination, as presented in the development of the EKF, proposed in next section.

The rotation matrix in terms of the quaternion elements is given by

$$A_q = \cdots$$
$$\begin{bmatrix} -1+2\begin{pmatrix} q_0^2 + \\ q_1^2 \end{pmatrix} & 2\begin{pmatrix} q_1q_2 - \\ q_0q_3 \end{pmatrix} & 2\begin{pmatrix} q_1q_3 + \\ q_0q_2 \end{pmatrix} \\ 2\begin{pmatrix} q_1q_2 + \\ q_0q_3 \end{pmatrix} & -1+2\begin{pmatrix} q_0^2 + \\ q_2^2 \end{pmatrix} & 2\begin{pmatrix} q_2q_3 - \\ q_0q_1 \end{pmatrix} \\ 2\begin{pmatrix} q_1q_3 - \\ q_0q_2 \end{pmatrix} & 2\begin{pmatrix} q_2q_3 + \\ q_0q_1 \end{pmatrix} & -1+2\begin{pmatrix} q_0^2 + \\ q_3^2 \end{pmatrix} \end{bmatrix}. \tag{34}$$

and substituting the matrix $Rot(\psi,\theta,\phi)$ by the quaternion matrix A_q, the matrix containing the baselines' local coordinates is given by

$$B_{NED} = A_qB_{xyz}. \tag{35}$$

Finally, the Euler angles can be obtained from the quaternion matrix as

$$\begin{aligned}\theta &= sin^{-1}\left(-A_q^{31}\right),\\ \phi &= tan^{-1}\left({A_q^{32}}/{A_q^{33}}\right),\\ \psi &= tan^{-1}\left({A_q^{21}}/{A_q^{11}}\right),\end{aligned} \tag{36}$$

where the superscript in the matrix represents its index.

2) Extended Kalman Filter

To obtain the Euler angles based on the rotation quaternion it is necessary to estimate the parameters q_0, q_1, q_2 and q_3. The system dynamics of the quaternion is represented by

$$\dot{q} = \frac{1}{2}\Omega q, \tag{37}$$

where q is the vector containing the quaternion components, that is, $q = [q_0\ q_1\ q_2\ q_3]^T$, and Ω is the skew-symmetric matrix, defined as

$$\Omega = \begin{bmatrix} 0 & \omega_z & -\omega_y & \omega_x \\ -\omega_z & 0 & \omega_x & \omega_y \\ \omega_y & -\omega_x & 0 & \omega_z \\ -\omega_x & -\omega_y & -\omega_z & 0 \end{bmatrix}, \tag{38}$$

where $\omega = \left[\omega_x\ \omega_y\ \omega_z\right]^T$ are the angular velocities in the body frame axis. In this paper only GPS observables and its derivations are used as observations. Thus, the angular velocities must be estimated along with the quaternion components.

The continuous system (37) leads to a linear time-varying discrete system defined as

$$x_{k+1} = F(x_k)_k + G_kw_k, \tag{39}$$

with each component being

$$x_{k+1} = \begin{bmatrix} q_{k+1} \\ \omega_{k+1} \end{bmatrix}, \quad (40)$$

$$F_k = \begin{bmatrix} q_k + \frac{1}{2}\Delta t \Omega_k q_k \\ \omega_k \end{bmatrix}, \quad (41)$$

$$G_k = \begin{bmatrix} -\frac{1}{2}\Xi & 0 \\ 0 & I \end{bmatrix}, \quad (42)$$

$$\Xi = \begin{bmatrix} q_3 & -q_2 & q_1 \\ q_2 & q_3 & -q_0 \\ -q_1 & q_0 & q_3 \\ -q_0 & -q_1 & -q_2 \end{bmatrix}, \quad (43)$$

where Δt is the sampling ($\Delta t = 1\ s$ for the GPS case), w_k is the process noise, Gaussian distributed with zero mean and covariance Q, and $\Xi\omega = \Omega q$, accordingly to [17].

The measurement model relates the baselines' coordinates with the quaternion elements estimated by the EKF and the known positions of the GPS antennas in the body fixed frame, accordingly to (35). Additionally, the measurement model takes into account the unitary norm constraint of the quaternion, defined in (33). This is done by using this constraint has a perfect measurement, as described in [18]. Thus, the measurement model is non linear time-varying and has the form

$$z_k = h(x_k)_k + v_k, \quad (44)$$

where v_k is the measurement noise, Gaussian distributed with zero mean and covariance R, and

$$z_k = \begin{bmatrix} b_{NED}^{12} \\ b_{NED}^{13} \\ b_{NED}^{14} \\ 1 \end{bmatrix}, \quad (45)$$

$$h(x_k)_k = \begin{bmatrix} A_q b_{NED}^{12} \\ A_q b_{NED}^{13} \\ A_q b_{NED}^{14} \\ q^T q \end{bmatrix}. \quad (46)$$

Since the observation model is non linear, to estimate the quaternion components and the angular velocities it is necessary to implement an EKF, which in this case consists in the linearization of the measurement model around the nominal solution. This is done by Taylor Series expansions, where neglecting the high order terms (assumed to have small numeric values), [19], leads to the Jacobian matrices defined as

$$H_k = \begin{bmatrix} \frac{\partial h(x_k)_k}{\partial q} & \frac{\partial h(x_k)_k}{\partial \omega} \end{bmatrix}. \quad (47)$$

The process noise characterizes the small disturbance in the system's dynamics and is given by, [19] and [20],

$$Q_k = E[w_k w_k^T] = \cdots$$
$$\int_{t_k}^{t_{k+1}} F(t_{k+1}, \tau) G(\tau) Q G^T(\tau) F^T(t_{k+1}, \tau)\, d\tau, \quad (48)$$

Where Q is a diagonal matrix containing the covariance of the disturbances present in the angular velocities, that is,

$$Q = \begin{bmatrix} Q_\omega & 0 \\ 0 & Q_{\omega_{bias}} \end{bmatrix}_{6\times 6}, \quad (49)$$

where Q_ω is the covariance of the angular velocity noise and $Q_{\omega_{bias}}$ is the covariance of the angular velocity bias noise, [17]. These two parameters must be tuned in order to obtain the best solution, but since it is not used any rate gyro, it is assumed that the value of $Q_{\omega_{bias}}$ is close to zero. To solve (48) it is assumed that the time interval between two measurements is small enough to use the approximation

$$Q_k \approx G_k Q G_k^T \Delta t. \quad (50)$$

Since the measurements used are the coordinates of the baseline vectors (assumed to be independent), the measurement covariance matrix of each baseline is diagonal, with each component being the correspondent variance. Thus for the three baselines and the quaternion norm perfect measurement (noise free), the observation covariance matrix of the EKF is defined as

$$R_k = E[v_k v_k^T] = \cdots$$
$$\begin{bmatrix} R_{NED}^{12} & 0 & 0 & 0 \\ 0 & R_{NED}^{13} & 0 & 0 \\ 0 & 0 & R_{NED}^{14} & 0 \\ 0 & 0 & 0 & 0 \end{bmatrix}, \quad (51)$$

where $R_{NED} = \begin{bmatrix} \sigma_N^2 & 0 & 0 \\ 0 & \sigma_E^2 & 0 \\ 0 & 0 & \sigma_D^2 \end{bmatrix}$ for the respective baseline.

Finally, the EKF has the form

$$\hat{x}_k^- = F(x_k)_k, \quad (52)$$

$$P_k^- = F_k P_{k-1} F_k^T + Q_k. \quad (53)$$

$$K_k = P_k^- H_k^T \left(H_k P_k^- H_k^T + R_k\right)^{-1}, \quad (54)$$

$$\hat{x}_k = \hat{x}_k^- + K_k(z_k - h(\hat{x}_k^-)_k), \quad (55)$$

$$P_k = (I - K_k H_k) P_k^-, \quad (56)$$

where the state vector and the respective covariance matrix, estimated in the previous instant, are propagated to the new time instant in equations (52) and (53), respectively, which consist in the prediction step. The remaining equations correspond to the update step, where the Kalman gain is determined (equation (54)) and is used to weight the state prediction based on the innovation process in equation (55). In equation (56) the new error covariance matrix is obtained.

The developed EKF can provide a solution for the problem at hand and is unique.

V. Solution Implementation

A. GPS Receivers

To test the solutions previously discussed, several tests were carried out using four Magellan AC12 GPS receivers, in order to process carrier-phase and code raw measurements.

One U-Blox 6 GPS receiver was used in order to obtain the ephemerides and the ionospheric correction parameters of the satellites.

The communication with each GPS receiver was made using RS-232 interface.

B. Algorithm Overview

The techniques presented in this paper were implemented accordingly to the algorithm depicted in Figure V.1, which was developed in MatLab.

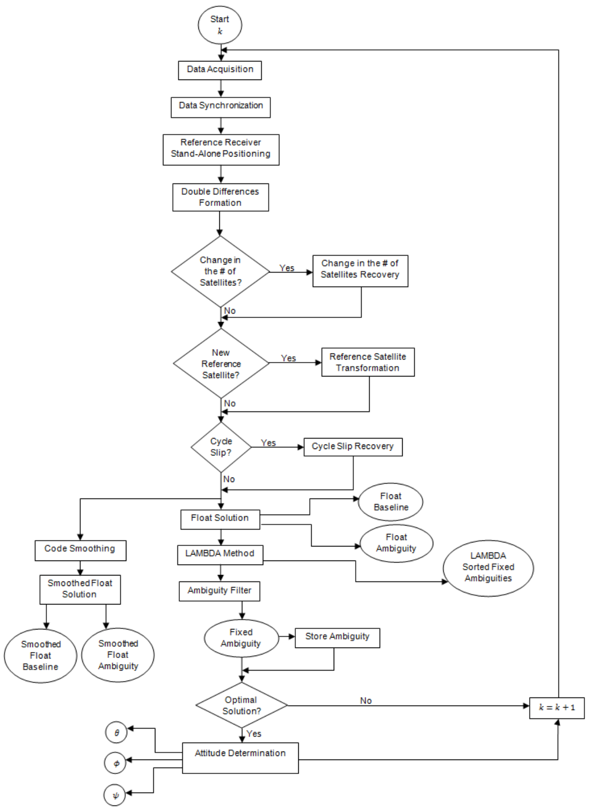

Figure V.1 – Flowchart of the developed algorithm

It is important to note that multiple solutions are obtained for the integer ambiguity and hence for the baseline vector, such as the float solution, the smoothed float solution, the LAMBDA method solution and the Ambiguity Filter solution. In the results section a comparison between the different solutions is presented.

C. Single Baseline Trial Description

The objective of the single baseline trial is the performance evaluation of the Ambiguity Filter, in a static scenario with low levels of multipath. The distance between the two GPS antennas that define the baseline vector is $10.665\ m$, and are placed at the same height (i.e. it is expected that the baseline's Up coordinate is close to zero).

D. Multiple Baseline Trial Description

The combination of multiple baselines is intended evaluate the performance of the Ambiguity Filter in a scenario with higher levels of multipath and to validate the attitude determination techniques. For that, receivers were installed in the top of a car (at known fixed positions in the vehicle's frame) as depicted in Figure V.2, where the baseline 1-4 is pointing to the moving direction. The length of each baseline was: $\|b_{1-2}\| = \|b_{1-3}\| \approx 0.8\ m$ and $\|b_{1-4}\| \approx 1.35$.

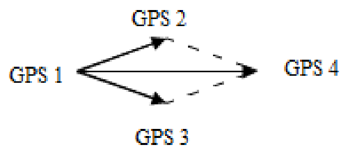

Figure V.2 – GPS receivers' disposition

Those tests were made in two different scenarios: static and dynamic. It is expected that the Up coordinate is close to zero for the static trial and during the initial epochs of the dynamic trial. The respective results will be presented in the next subsections.

Note that the term "Baseline 1-n" stands for the baseline vector between the GPS receiver 1 and the GPS receiver n.

VI. Results

A. Single Baseline – Static Trial Results

The first exercise is the comparison between the two metrics of the Ambiguity Filter, described in Section III.D.1). As depicted in Figure VI.1, the solution obtained using metric 2 has better performance than the solution obtained using metric 1, since converges more quickly to the correct solution. However, in this case both solutions obtained after stabilization are correct.

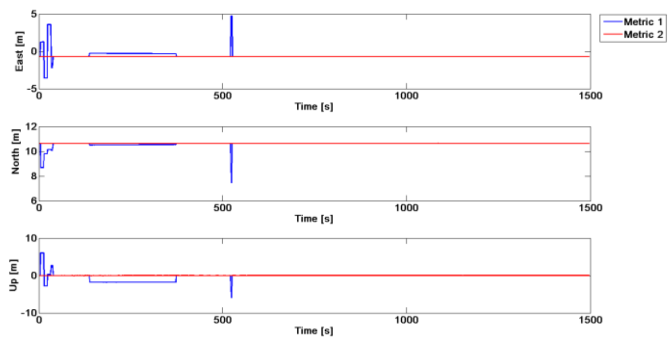

Figure VI.1 – Baseline ENU coordinates evolution, using the Ambiguity Filter metrics 1 and 2 to solve the integer ambiguity problem for the single baseline static trial

The high precision level of solution obtained by the Ambiguity Filter is emphasized when compared with the solutions obtained without the correct integer ambiguity, that is, the float solution, the smoothed float solution and the

LAMBDA method solution. This fact is illustrated by comparing the solutions present in Figure VI.2 and the statistical performance of each technique depicted in Table 1.

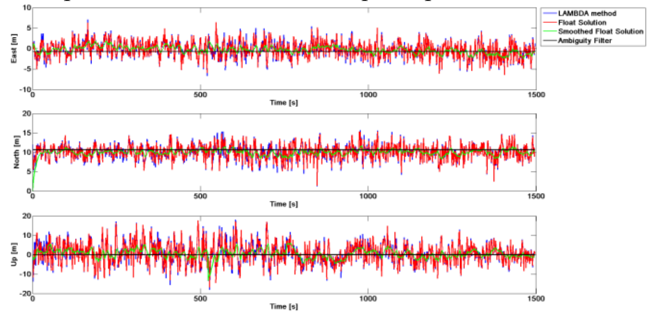

Figure VI.2 – Baseline ENU coordinates evolution using different techniques to solve the integer ambiguity problem

Table 1 – Performance of the baseline ENU coordinates in the single baseline static trial using different techniques to solve the integer ambiguity problem

	Ambiguity Filter	LAMBDA method	Float Solution	Smoothed Float Solution
μ_{East} (m)	−0.713	−0.371	−0.346	−0.327
σ_{East} (m)	0.002	1.953	1.889	0.804
μ_{North} (m)	10.636	9.981	9.977	9.935
σ_{North} (m)	0.002	1.878	1.809	0.816
μ_{Up}(m)	0.007	0.446	0.414	0.408
σ_{Up} (m)	0.007	5.311	5.149	2.247

Comparing the different results, it is clear that the Ambiguity Filter allow a better precision (millimeter-level) than the remaining techniques, and hence is the best technique to use regarding precise attitude determination.

The similarity between the LAMBDA method solution and the float solution is due to the fact that the float solution is used as the centre point of the search process made by the LAMBDA method. Thus, the best solution in this method's sense is the one that is the integer nearest to the centre of the search space, which is the float solution.

B. Multiple Baselines – Static Trial Results

The primary objective was to test both metrics of the Ambiguiy Filter, defined in III.D.3). For that purpose, it is presented the baseline 1-4 ENU coordinates evolution, for both metrics. From the results depicted in Figure VI.3 it is clear that only the solution obtained by using metric 2 converges to the correct solution, which is the one that converges to a Up coordinate close to zero. This fact is confirmed in Table 2, where the statistical performance of the three baselines' Up coordinate is depicted. For baselines 1-2 and 1-3, the correct solution is achieved using both metrics, since the obtained Up coordinates are close to zero. However, for baseline 1-4 the solution using metric 1 does not stabilize in the correct integer ambiguity set, since the Up coordinate is nearly $-0.4\ m$. For metric 2 the baseline 1-4 stabilizes on the expected value for the Up coordinate. So, in this case metric 2 had a better performance than metric 1 in integer ambiguity resolution. Since the metric 2 is the one with best performance, a zoomed version of the Up coordinate of each baseline is depicted in Figure VI.4.

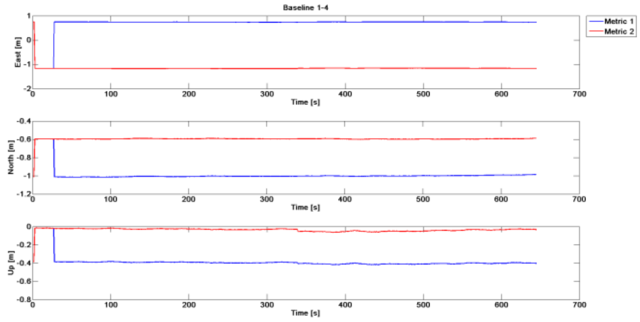

Figure VI.3 – Baseline 1-4 ENU coordinates, using the Ambiguity Filter metrics 1 and 2 to solve the integer ambiguity problem for the multiple baselines static trial

Table 2– Baselines' Up coordinate statistical performance (mean and standard deviation), after stabilization

		Baseline 1-2	Baseline 1-3	Baseline 1-4
Metric 1	μ (m)	−0.005	−0.009	−0.399
	σ (m)	0.015	0.01	0.009
Metric 2	μ (m)	−0.005	−0.009	−0.036
	σ (m)	0.015	0.01	0.012

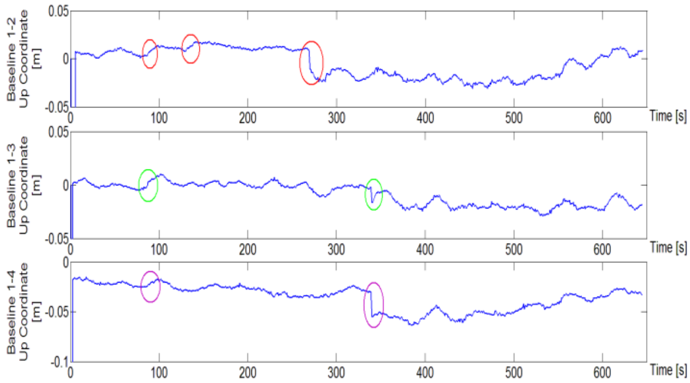

Figure VI.4 – Up coordinate, for baselines 1-2, 1-3 and 1-4, using metric 2

The colored ellipses in the plots of Figure VI.4 highlights how the baseline coordinates react when the number of visible satellites change, which is visible in Figure VI.5. In the baseline 1-3, the first change in the constellation does not have a visible effect on the basline's Up coordinate. When the effect of this changes can be noticed, it is only centimeter-level, which is an improvement when compared with the results presented in [9].

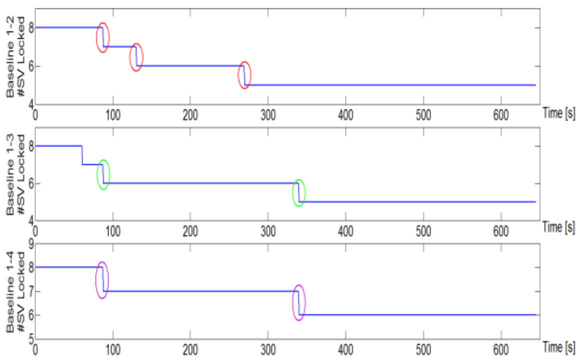

Figure VI.5 – Number of SVs used to compute the observables

Based on these results, metric 2 was selected to be used in the remaining tests.

Using multiple baselines, as represented in Figure V.2, and after the optimal integer ambiguity set is known for all the baselines, the attitude angles are obtained, accordingly with the techniques presented in Section IV.B. Thus, the obtained attitude angles for the static test are depicted in Figure VI.6.

As represented in Table 3 and in Figure VI.6, the heading angle is the one with best performance. This can be understood from the strong influence of the Up coordinate (noisier than the East and North) in both pitch and roll.

It is possible to see that both solutions, using the Rotation Matrix or the EKF, are similar. However, the solution obtained through time by the EKF is smoother, which is expected due to the recursive nature of the EKF.

Table 3 – Attitude angles' statistical performance for the static trial

		Rotation Matrix	Quaternion Based EKF
Pitch Angle	μ (°)	-0.666	-1.007
	σ (°)	1.001	0.708
Roll Angle	μ (°)	0.277	0.147
	σ (°)	0.709	0.751
Heading Angle	μ (°)	-115.193	-117.008
	σ (°)	0.261	0.212

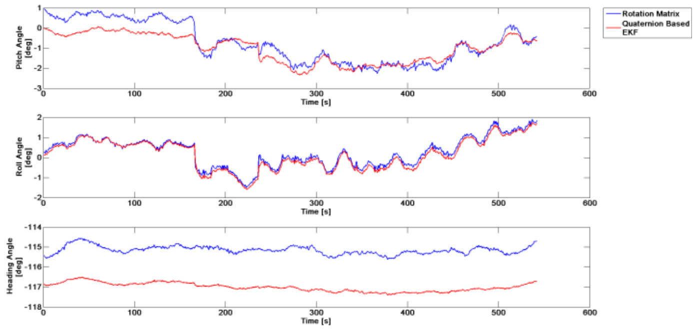

Figure VI.6 – Attitude angles for the static trial

C. *Multiple Baselines – Dynamic Trial Results*

For the dynamic trial, the car used as the test platform made a small path where variations of pitch and roll were mainly due to road irregularities, as depicted in Figure VI.7.

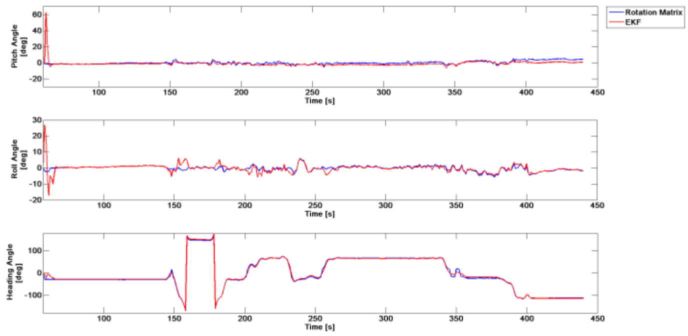

Figure VI.7 – Attitude angles for a dynamic trial

Before the car start moving (before $t = 150\ s$ and while the heading is still constant) pitch and roll angles are less corrupted by noise when compared with the phase where the car was in movement, as expected. It is important to notice that just before the epoch $t = 250\ s$, when the vehicle's heading was close to $-30°$, the roll angle increase is due to an inclination imposed to the vehicle (approximately $6°$, as illustrated by the zoom in Figure VI.9), proving that the attitude variation is well detected.

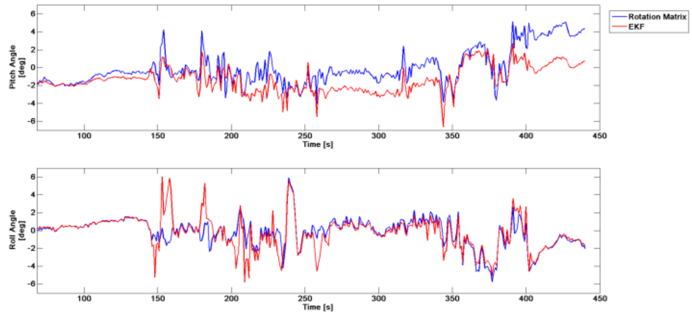

Figure VI.8 – Zoom of pitch and roll angles obtained with the rotation matrix technique and with the quaternion based EKF, for the dynamic trial

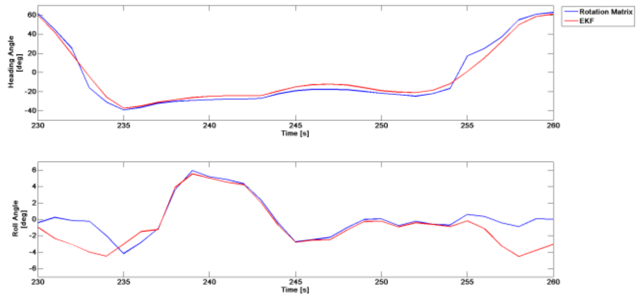

Figure VI.9 – Zoom of heading and roll angles, during a positive rotation about the $\boldsymbol{x}$ axis (positive roll angle) during the dynamic trial

By analyzing Figure VI.8, one may verify that at the beginning of the trajectory, around epoch $t = 150\ s$, the roll angle estimated by the EKF is highly disturbed when compared with the solution obtained by the rotation matrix. This fact is emphasized by the x term of the angular velocity after the platform start moving in Figure VI.10, which is not exact since the maneuvers made during the trial were with small accelerations. This may be explained by the decrease of precision in the Up coordinate after the platform started moving. This could be improved by using an accelerometer output as measurement of the EKF and hence to better estimate the angular velocities.

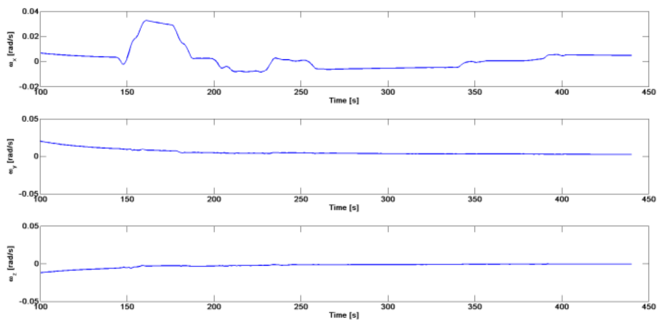

Figure VI.10 – Evolution of the angular velocities estimated by the EKF during the dynamic trial

VII. CONCLUSIONS

The static trial showed that the use of the LAMBDA method along with the Ambiguity Filter allows higher confidence in the determination of the correct integer ambiguity, and hence a millimeter level precision in the determination of the baseline vector.

The results for single and multiple baselines, in a static scenario, showed that the proposed improvements within the Ambiguity Filter offer an increase of this algorithm's accuracy. The metric 2 offered more confidence in determining the correct integer ambiguity than the metric 1. The introduction of a technique able to keep the correct integer ambiguity solution despite the variation in the satellites' constellation is another improvement within the Ambiguity Filter. This technique avoids resetting the algorithm and hence the restart of the search process for the integer ambiguity determination The results showed that, despite some oscillations due to variations in the satellites' constellation, it is possible to obtain a millimeter level precision, and hence a precision smaller than $1°\,(1\sigma)$ in the determination of the Euler angles.

For the attitude determination techniques, the static trial results showed that resorting to both the algorithm using the rotation matrix and the quaternion based EKF, it was possible to estimate the Euler angles with precisions smaller than $1°$ (1σ). However, the quaternion based EKF showed slight improvements regarding the estimation of both pitch and heading angles with an increased precision in the order of approximated $0{,}3°$ and $0{,}05°$, respectively, which is understandable since it is a recursive estimation algorithm.

Despite the disturbances augmentation, the dynamic results are representative of the successfully implementation of the attitude determination algorithms, capable of detecting attitude variations along the path made by the test platform. This fact was visible in the detection of a positive roll angle (of approximately 6°), imposed by climbing a sidewalk with the test vehicle. The increase in the level of disturbances is visible in the attitude angles that are function of the Up coordinate (which is more sensible to noise), that is, pitch and roll angles. For the EKF the roll angle is more affected by this phenomenon, since the highly disturbed Up coordinate led to a highly disturbed angular velocity about the x axis. However these disturbances do not affect the correct determination of the Euler angles, which is proved by the performance of the EKF innovation. Despite the disturbances' augmentation, the innovation has errors in the order of the centimeter (1σ).

Despite the good results presented in this paper, there are topics that could be addressed in future work. Such topics are related with the study of new improvements within the Ambiguity Filter and in the estimation of the attitude angles. Also new hardware features (such as INS sensors) could be added to the system, in order to couple the baseline measurements with different data, allowing the improvement in accuracy and precision of the Euler angles.

REFERENCES

[1] B. L. V. Kuylen, P. Nemry, F. Boon, A. Simsky, and J. F. M. Lorga, "*Comparison of Attitude Performance for Multi-Antenna Receivers,*" *European Journal of Navigation*, vol. 4, nº2, pp. 1-9, May 2006.

[2] E. D. Kaplan and C. J. Hegarty, *Understanding GPS: principles and applications*, 2nd ed. Artech House Publishers, 2006.

[3] P. Misra and P. Enge, *Global Positioning System : Signals , Measurements , and Performance*, 2nd ed. Ganga-Jamuna Press, 2006.

[4] P. Teunissen, "*Least-Squares Estimation of the Integer GPS Ambiguities,*" *Delft Geodetic Computing Centre LGR series*, No. 6, 16pp.

[5] P. J. D. Jonge, C. C. J. M. Tiberius, and P. J. G. Teunissen, "*Computational Aspects of the LAMBDA Method for GPS Ambiguity Resolution,*" *Proceedings of ION GPS-96, 9th International Technical Meeting of the Satellite Division of the Institute of Navigation, Kansas City, Missouri*, Sept. 17-20, pp 935-944.

[6] G. Strang and K. Borre, *Linear algebra, geodesy, and GPS*. Wellesley Cambridge Pr, 1997.

[7] P. Teunissen, "*The LAMBDA Method for the GNSS Compass,*" *Artificial Satellites-Journal of Planetary Geodesy,* Vol. 41, nº 3, pp 89-103, 2006.

[8] G. Giorgi and P. J. G. Teunissen, "*Carrier Phase GNSS Attitude Determination with the Multivariate Constrained LAMBDA Method,*" *IEEE Aerospace Conference, Big Sky, MT*, pp. 1-12, Mar. 2010.

[9] J. Reis, "*Real-time GPS Heading Determination,*" MSc Thesis, Instituto Superior Técnico, Technical University of Lisbon, November 2009.

[10] J. Reis, J. Sanguino, and A. Rodrigues, "*Baseline Influence on Single-Frequency GPS Precise Heading Estimation,*" in *Wireless Personal Communications Journal*, Springer Netherlands, 2012.

[11] J. Reis, J. Sanguino, and A. Rodrigues, "*Impact of Satellite Coverage in Single-Frequency Precise Heading Determination,*" in *Position Location and Navigation Symposium (PLANS), IEEE/ION*, 2010, Indian Wells, USA, 3-6 May 2010, pp. 592-597.

[12] J. Reis, J. Sanguino, and A. Rodrigues, "*Influence of Baseline Length in Single-Frequency Real-Time Vehicle Heading Estimation,*" in *The 13th International Symposium on Wireless Personal Multimedia Communications (WPMC)*, Recife, Brazil, 11-14 October 2010.

[13] R. E. Kalman, "A New Approach to Linear Filtering and Prediction Problems," *Transactions of the ASME - Journal of Basic Engineering,* vol. 82, no. Series D, pp. 35-45, 1960.

[14] F. V. Graas and M. Braasch, "GPS Interferometric Attitude and Heading Determination: Initial Flight Test Results," *The Institute of Navigation*, vol. IV, pp. 359-378, 1991.

[15] D. Kim and R. B. Langley, "*GPS Ambiguity Resolution and Validation : Methodologies , Trends and Issues,*" *in International Symposium on GPS/GNSS*, Seoul, Korea, 2000.

[16] J. B. Kuipers, *Quaternions and rotation sequences*, vol. 1. Princeton university press Princeton, NJ, 1999

[17] Y. T. Chiang, L. S. Wang, F. R. Chang, and H. M. Peng, "Constrained Filtering Method for Attitude Determination using GPS and Gyro," *IEE Proceedings - Radar, Sonar and Navigation*, vol. 149, no. 5, p. 258, 2002.

[18] D. Simon, *Optimal state estimation: Kalman, H [infinity] and nonlinear approaches*. John Wiley and Sons, 2006.

[19] Y. Bar-Shalom, X. Li, and T. Kirubarajan, *Estimation with applications to tracking and navigation*, vol. 9. 2001.

[20] F. Nunes, Lecture Notes on: "Sistemas de Controlo de Tráfego," 2010.